International Journal of Scientific Research in Engineering and Management (IJSREM)
Volume: 09 Issue: 11 | Nov - 2025 SJIF Rating: 8.586 ISSN: 2582-3930

Dynamic Analysis of Vertical Irregular Reinforced Concrete Buildings: Evaluating Blast Resistance and Soft Storey Vulnerabilities

Swapnil Namdev Doud[1], DR. DB Mohite[2]

[1]Scholer, Dr. Babasaheb Ambedkar Technological University, Lonere-Raigad Maharashtra

[2]Associate professor, Dr. Babasaheb Ambedkar Technological University, Lonere-Raigad Maharashtra

Abstract

The increasing occurrence of explosions from terrorism, industrial accidents, and military conflicts has highlighted the vulnerability of high-rise buildings to blast-induced forces. Traditional reinforced concrete (RCC) structures are primarily designed for static loads and often lack adequate resilience against dynamic, short-duration blast loads. This study focuses on the dynamic analysis of vertical irregular RCC buildings, specifically G+15, G+20, and G+25 structures, incorporating soft-storey configurations that are known to be highly susceptible to damage under impulsive loads. Blast loads are calculated following IS 4991:1968 and TM5-1300 standards, considering parameters such as peak overpressure, impulse duration, and standoff distance. The structural behavior under these loads is modeled and analyzed using ETABS through time-history simulations and finite element analysis (FEA). The study evaluates critical response parameters including displacement, inter-storey drift, shear forces, and base shear, comparing regular and irregular building configurations under varying blast scenarios. Results indicate that soft-storey irregularities significantly amplify deformations and drifts, particularly at lower floors and under closer blast proximity. The findings highlight the importance of strategic reinforcement, optimal shear wall placement, and material enhancements to improve blast resistance. This research provides valuable insights for designing safer and more resilient high-rise structures, contributing to enhanced structural performance in high-risk zones and informing guidelines for blast-resistant design in vertical irregular buildings.

Keywords: Blast Resistance, Vertical Irregular Buildings, Reinforced Concrete (RCC), Soft-Storey Structures, Dynamic Analysis

I. INTRODUCTION

The increasing frequency and intensity of explosions, resulting from terrorism, industrial accidents, and military conflicts, have raised significant concerns regarding the vulnerability of buildings to blast-induced forces. Traditional buildings, primarily designed to withstand static loads such as dead and live loads, are often inadequate in coping with the dynamic and short-duration forces generated by blasts. Among various types of buildings, high-rise reinforced concrete (RCC) structures, particularly those with vertical irregularities such as soft storeys, are especially prone to severe damage under blast loading. Vertical irregularities in buildings, where certain floors are significantly weaker than others, increase the susceptibility to dynamic loads, making the design and analysis of such structures crucial for ensuring their safety in high-risk zones. Soft storey conditions, which refer to floors that are much weaker in lateral stiffness compared to the floors above and below them, significantly affect a building's response to dynamic forces. In the event of an explosion, the imbalance in lateral stiffness causes excessive displacement and drift at the soft storey, leading to potential collapse or severe damage. Such irregularities are common in high-rise buildings, particularly in older structures or those built without considering blast resistance in their design. Understanding how these structures respond to blast loads, especially in terms of deformation, drift, and shear forces, is therefore critical to developing effective solutions for improving their resilience.

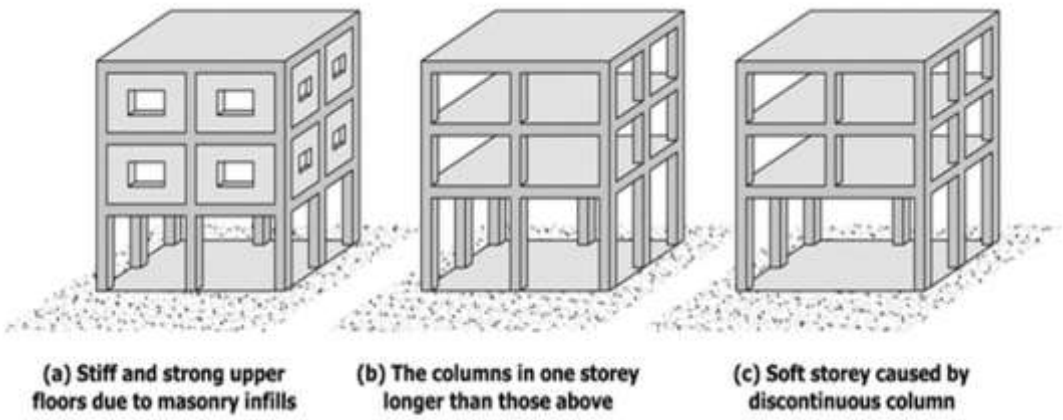

Figure 1. Effects of Column Discontinuity on Building Stiffness: (a) Stiff Upper Floors due to Masonry Infill, (b) Longer Columns in One Storey, (c) Soft Storey due to Discontinuous Column

The research presented in this paper focuses on the dynamic analysis of vertical irregular reinforced concrete buildings subjected to blast loads. Specifically, the study evaluates the vulnerability of G+15, G+20, and G+25 RCC buildings with soft storeys to blast-induced forces. The analysis uses advanced simulation tools such as Finite Element Analysis (FEA) and time-history simulations in ETABS to model the structural behavior of these buildings under varying blast scenarios. The study incorporates blast load calculations based on standards like IS 4991 and TM5-1300, which consider key parameters such as peak overpressure, impulse duration, and reflected pressure.

This research aims to provide comprehensive insights into the structural response of high-rise buildings under blast loading, particularly focusing on the impact of vertical irregularities like soft storeys. The study also explores various design modifications and material enhancements to improve blast resistance, such as reinforcing lower floors, incorporating shear walls, and using blast-resistant materials. By focusing on the vulnerabilities associated with vertical irregularities and soft storeys, this research seeks to contribute valuable knowledge for the design of safer and more resilient buildings capable of withstanding explosive events.

II. LITERATURE REVIEW

The dynamic analysis of vertical irregular buildings, particularly those with reinforced concrete (RC) structures, has been a focal point of recent research due to the growing concerns about their performance under extreme loading conditions such as wind, seismic, and blast forces. Vertical irregularities in buildings, characterized by variations in mass, stiffness, and geometry, significantly impact the dynamic behavior, making them more susceptible to structural failure during events like earthquakes and explosions. This literature review synthesizes key studies examining the effects of vertical irregularities on building performance, with an emphasis on dynamic responses and structural vulnerabilities.

HB Akhilesh et al. (2020) conducted a dynamic analysis of vertical irregular tall structures under wind loads, using ETABS and IS 16700: 2017 provisions. The study modeled buildings with varying cantilevered offsets and plan dimensions, analyzing parameters like time period, frequency, storey displacement, and drift. The study found that vertical irregularities amplify the dynamic response, especially under high-intensity wind forces, and emphasized the need for specialized design approaches for these buildings. Their regression analysis highlighted that vertical irregularity leads to greater structural displacement and drift, urging the integration of more resilient features in the design of tall buildings. Similarly, **Mohammadismail S Memon et al. (2021)** explored the seismic performance of RC buildings with vertical irregularities. They analyzed the impact of mass and geometric irregularities on multi-storey buildings, using STAAD ProV8i SS6 software for simulation. The study highlighted how the uneven distribution of mass and stiffness in buildings increases the vulnerability to seismic forces, leading to larger bending moments, node displacements, and shear forces in buildings with irregularities compared to regular structures. Their results underlined the importance of accounting for vertical irregularities in seismic design to prevent catastrophic failures during earthquakes. **Harsha N R et al. (2023)** expanded the scope of analysis by studying the seismic performance of buildings with vertical irregularities with and without lateral force-resisting systems. Their study utilized ETABS to simulate buildings with varying levels of irregularities, comparing displacement and shear forces in seismic zone V. They found that lateral force-resisting systems, such as bracings and dampers, significantly enhanced the seismic performance of irregular buildings by reducing displacement and improving storey shear, thereby suggesting the use of such systems in high-risk seismic zones.

In a similar vein, **Basu Dhakal et al. (2023)** examined the seismic performance of buildings with vertical and planar irregularities using ETABS, following NBC 105:2020 guidelines. They compared the seismic responses of regular and irregular buildings and found that irregular buildings experienced more significant deformations and drifts, underscoring the need for robust design measures. Their study also emphasized that incorporating shear walls and optimizing the placement of lateral force-resisting systems can improve the seismic resilience of irregular buildings. **Kyoung Min Ro et al. (2021)** focused on simplifying the modeling of vertically irregular structures for dynamic assessment. They proposed a method to convert irregular structures into geometrically regular models using a stiffness equation. Their comparison of traditional and simplified models revealed minimal differences in dynamic response, suggesting that the simplified approach can provide accurate predictions for story shear and drift, particularly in early-stage design processes. Further research by **D. Annapurna et al. (2023)** also explored seismic performance, focusing on irregularities such as mass and stiffness variations. Their study used the Response Spectrum method to assess story displacement, drift, shear, and stiffness across different seismic zones. The findings indicated that irregular buildings experience higher lateral loads and more pronounced story displacement, particularly in higher seismic zones, reinforcing the need for tailored design approaches based on regional seismicity. Lastly, **Srinidhi G et al. (2022)** investigated the role of shear walls in improving the seismic behavior of vertically irregular buildings. Their study emphasized the optimal placement of shear walls, particularly in irregular layouts such as I-frame and L-frame structures. The findings highlighted that proper shear wall placement significantly reduces displacement, drift, and shear forces, thus enhancing the overall seismic performance of irregular buildings.

2.1 Research gap

While existing studies have examined the seismic and wind response of vertically irregular buildings, particularly focusing on their displacement, drift, and shear forces, a comprehensive understanding of their behavior under blast loads remains limited. Many studies have explored the impact of vertical irregularities such as mass and stiffness variations, but the specific vulnerabilities of soft storeys in blast-resistant design are under-researched. Additionally, while dynamic analysis methods like FEA are widely used, few studies integrate real-time data or adaptive systems for improving the blast resistance of irregular buildings. There is a need for more focused research on enhancing the resilience of vertically irregular buildings under extreme dynamic loading scenarios.

III. RESEARCH METHODOLOGY

The methodology of this study aims to investigate the structural response of G+15, G+20, and G+25 Reinforced Concrete (RCC) buildings subjected to blast loads. The study integrates blast load calculations, dynamic simulations, and Finite Element Analysis (FEA) to evaluate the buildings' performance under explosive forces.

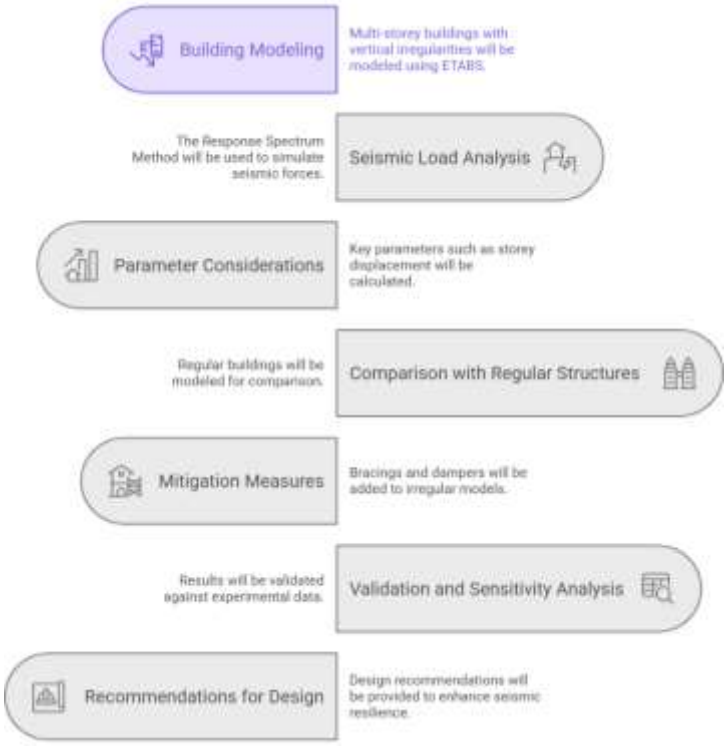

Figure 2: Methodology Flowchart

1. Blast Load Calculation:

Blast loads are determined following the guidelines of IS 4991 and TM5-1300. Key parameters such as peak overpressure, impulse duration, and reflected pressure are computed using the scaled distance formula, which accounts for the distance from the blast source and the explosive charge weight. The TNT equivalent energy is calculated, and these values are applied to simulate blast effects on the buildings.

2. Dynamic Simulation:

Structural models of the buildings, including reinforcement detailing, material properties, and layout, are developed in ETABS. Time-history dynamic simulations are performed to capture the structural response under blast loads. Critical parameters such as displacement, inter-storey drift, shear forces, and overturning moments are assessed for each model under various blast scenarios.

3. Model Validation:

The accuracy of the simulation results is verified against experimental data or established benchmarks from prior studies. This step ensures that the numerical models reliably replicate the structural behavior under blast conditions.

4. Analysis and Recommendations:

Simulation results are analyzed to identify vulnerable regions and critical structural weaknesses. Based on these insights, design recommendations are formulated to enhance the blast resistance, including possible material enhancements, reinforcement modifications, and layout optimizations.

IV. DESIGN AND MODELLING

The design and modeling of G+15, G+20, and G+25 RCC buildings subjected to blast loads involve defining building geometry, including storey heights, number of floors, and material properties. Each building is modeled as a moment-resisting frame, with conventional reinforcement detailing, while soft-storey conditions are incorporated in the lower floors to simulate realistic vulnerabilities. Finite Element Analysis (FEA) is conducted in ETABS, representing structural components—beams, columns, slabs, and shear walls—with appropriate elements. Material properties include M30 grade concrete and Fe500 steel, with corresponding modulus of elasticity, yield strength, and Poisson's ratio. This setup enables evaluation of key responses such as displacement, drift, shear forces, and overturning moments under blast loading scenarios.

V. PROBLEM STATEMENT

This study examines the structural performance of G+15, G+20, and G+25 reinforced concrete (RCC) buildings subjected to blast loads, with particular emphasis on soft-storey irregularities and non-uniform shear wall distribution. Following the IS:4991–1968 guidelines, both regular and irregular building models are developed in ETABS to evaluate their vulnerability to blast-induced damage. The research underscores the importance of incorporating blast loading alongside conventional gravity and seismic forces, especially for structures in high-risk or sensitive areas, such as government buildings, embassies, and critical infrastructure, to ensure structural safety and enhance resilience against sudden impulsive forces.

- **Beam sizes:**
  - 300 mm × 500 mm (up to 11th storey)
  - 250 mm × 450 mm (top 4 storeys)
- Bay size: 3.15 m × 3.9 m
- Storey height: 3.6 m
- Grid Size 12m x 12m
- Slab thickness: 120 mm

Table 1: Storey Drift and Standoff Distance for Regular and Irregular Structures

TYPE	**REGULAR STRUCTURE**		
MODEL	**STANDOFF DISTACE m**		
G+15	10	15	20
G+20	10	15	20
G+25	10	15	20
TYPE	**IRREGULAR STRUCTURE**		
MODEL	**STANDOFF DISTACE m**		
G+15	10	15	20
G+20	10	15	20
G+25	10	15	20

As Mentioned in Above table, Total 18 models are analysed for TNT load 100 kg, Blast Load calculations are done using IS 4991 and later applied in ETABS

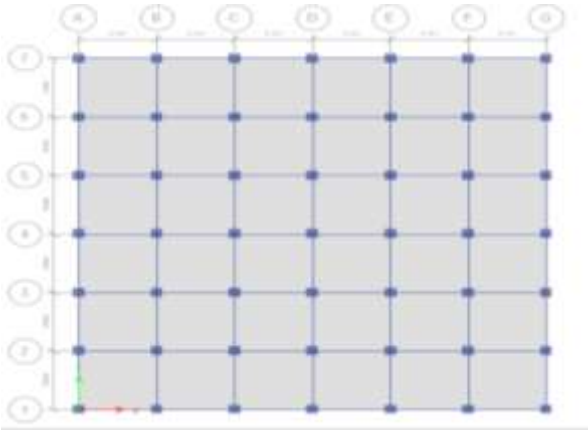

Figure 3: Storey Drift Analysis in EQ Y for Various Structural Scenarios

VI. Blast Load Calculation Based on IS:4991–1968

IS 4991:1968 provides guidance for calculating blast overpressures resulting from an explosion and converting them into equivalent static forces for structural design.

1. Scaled Distance (Z)

$$Z = \frac{R}{W^{1/3}}$$

Where:

- R = standoff distance (m)
- W = weight of TNT (kg)
- Z = scaled distance (m/kg$^{1/3}$)

CASE 1: 100 kg TNT @ 10 m

Step 1: Scaled Distance Z

$$Z = \frac{R}{W^{1/3}} = \frac{10}{4.64} = 2.155$$

Step 2: Peak Reflected Pressure P_r

From blast chart at $Z = 2.15$:

$$P_r \approx 330.48\,\text{kN/m}^2$$

Step 3: Max Time t_d

From time-vs-Z chart for Z = 2.15:

$$t_d \approx 0.0036\,\text{sec}$$

CASE 2: 100 kg TNT @ 20 m

Step 1: Scaled Distance Z

$$Z = \frac{20}{4.64} = 4.31$$

Step 2: Peak Reflected Pressure P_r

From chart at $Z = 4.31$:

$$P_r \approx 148.08\,\text{kN/m}^2$$

Step 3: Max Time t_d

From chart at Z = 4.31:

$$t_d \approx 0.0068 \text{ sec}$$

CASE 3: 100 kg TNT @ 30 m

Step 1: Scaled Distance Z

$$Z = \frac{30}{4.64} = 6.47$$

Step 2: Peak Reflected Pressure P_r

From blast pressure chart at Z = 6.47:

$$P_r \approx 77 \text{ kN/m}^2$$

Step 3: Max Time t_d

From positive phase duration chart at Z = 6.47:

$$t_d \approx 0.0096 \text{ sec}$$

Table 2: Blast Impact Data for Different Distances

Case	Distance R (m)	$Z = \frac{R}{4.64}$	Pro (kN/m²)	Max Time (sec)
100 kg @ 10 m	10.0	2.155	330.48	0.0036
100 kg @ 20 m	20.0	4.310	148.08	0.0068
100 kg @ 30 m	30.0	6.470	77.00	0.0096

2. Peak Overpressure (Pr) Estimation

From IS 4991 Table 1 or UFC 3-340-02 chart (for Z = 2.15 m/kg$^{1/3}$):

- Peak overpressure (Pr) ≈ 138 kPa
- Positive phase duration (td) ≈ 6.5 ms
- Impulse (I) ≈ 480 kPa·ms

3. Equivalent Static Pressure (Peq)

As per IS:4991, the blast load can be modeled as an equivalent triangular load:

$$P_{eq} = 0.5 \times P_r$$

$$P_{eq} = 0.5 \times 138 = 69 \text{ kPa}$$

This is applied on the blast-exposed surface (typically ground floor exterior walls or façade).

4. Blast Load (Force) on Shear Wall

Assume exposed area (A) of a typical wall:

$$A = H \times L = 3.6 \times 21 = 75.6 \text{ m}^2$$

$$F = P_{eq} \times A = 69 \times 75.6 = 5{,}216.4 \text{ kN}$$

This force is applied as lateral load on the first storey shear wall in the ETABS model.

Table 3: Floor-wise Blast Impact Force Calculation

Floor	Center_Height (m)	Distance R (m)	Scaled Distance Z	Pro (kN/m^2)	Area (m^2)	Force (kN)
1	1.5	30.04	6.47	80	2.7	216
2	4.5	30.34	6.54	80	2.7	216
3	7.5	30.92	6.66	80	2.7	216
4	10.5	31.78	6.85	80	2.7	216
5	13.5	32.9	7.09	80	2.7	216
6	16.5	34.24	7.38	80	2.7	216
7	19.5	35.78	7.71	80	2.7	216
8	22.5	37.5	8.08	80	2.7	216
9	25.5	39.37	8.48	80	2.7	216
10	28.5	41.38	8.91	80	2.7	216
11	31.5	43.5	9.37	80	2.7	216
12	34.5	45.72	9.85	95	2.4	228
13	37.5	48.02	10.35	95	2.4	228
14	40.5	50.4	10.86	95	2.4	228
15	43.5	52.84	11.38	95	2.4	228

Table 3 presents the floor-wise blast impact forces on a multi-storey building. The center height and corresponding distance from the blast source are used to calculate the scaled distance (Z). Blast pressures (Pro) and floor areas determine the impact force on each floor. Lower floors experience 216 kN due to uniform pressure of 80 kN/m², while upper floors (12–15) see slightly higher forces (228 kN) from increased pressure (95 kN/m²) despite larger distances, reflecting variations in blast intensity with height.

Table 4: Floor-wise Blast Load Impact Analysis

Floor	Center_Height (m)	Distance R (m)	Scaled Distance Z	Pro (kN/m^2)	Area (m^2)	Force (kN)
1	1.5	30.04	6.47	80	2.7	216
2	4.5	30.34	6.54	80	2.7	216
3	7.5	30.92	6.66	80	2.7	216
4	10.5	31.78	6.85	80	2.7	216
5	13.5	32.9	7.09	80	2.7	216
6	16.5	34.24	7.38	80	2.7	216
7	19.5	35.78	7.71	80	2.7	216
8	22.5	37.5	8.08	80	2.7	216
9	25.5	39.37	8.48	80	2.7	216
10	28.5	41.38	8.91	80	2.7	216
11	31.5	43.5	9.37	80	2.7	216
12	34.5	45.72	9.85	80	2.7	216
13	37.5	48.02	10.35	80	2.7	216
14	40.5	50.4	10.86	80	2.7	216
15	43.5	52.84	11.38	80	2.7	216
16	46.5	55.34	11.92	80	2.7	216
17	49.5	57.88	12.47	105	2.4	252
18	52.5	60.47	13.03	105	2.4	252

19	55.5	63.09	13.59	105	2.4	252
20	58.5	65.74	14.16	105	2.4	252

Table 4 presents the floor-wise blast load impact on a 20-storey building. Using the center height and distance from the blast source, the scaled distance (Z) is calculated. Blast pressure (Pro) multiplied by floor area determines the force on each floor. Lower to mid floors (1–16) experience 216 kN with 80 kN/m² pressure, while upper floors (17–20) experience higher forces of 252 kN due to increased pressure (105 kN/m²), showing the variation of blast impact with height.

Table 5: Floor-wise Blast Impact Force and Pressure Analysis

Floor	Center_Height (m)	Distance R (m)	Scaled Distance Z	Pro (kN/m^2)	Area (m^2)	Force (kN)
1	1.5	30.04	6.47	80	2.7	216
2	4.5	30.34	6.54	80	2.7	216
3	7.5	30.92	6.66	80	2.7	216
4	10.5	31.78	6.85	80	2.7	216
5	13.5	32.9	7.09	80	2.7	216
6	16.5	34.24	7.38	80	2.7	216
7	19.5	35.78	7.71	80	2.7	216
8	22.5	37.5	8.08	80	2.7	216
9	25.5	39.37	8.48	80	2.7	216
10	28.5	41.38	8.91	80	2.7	216
11	31.5	43.5	9.37	80	2.7	216
12	34.5	45.72	9.85	80	2.7	216
13	37.5	48.02	10.35	80	2.7	216
14	40.5	50.4	10.86	80	2.7	216
15	43.5	52.84	11.38	80	2.7	216
16	46.5	55.34	11.92	80	2.7	216
17	49.5	57.88	12.47	80	2.7	216
18	52.5	60.47	13.03	80	2.7	216
19	55.5	63.09	13.59	80	2.7	216
20	58.5	65.74	14.16	80	2.7	216
21	61.5	68.43	14.74	80	2.7	216
22	64.5	71.14	15.33	100	2.5	250
23	67.5	73.87	15.91	105	2.4	252
24	70.5	76.62	16.51	110	2.4	264
25	73.5	79.39	17.1	110	2.4	264

Table 5 shows the floor-wise blast impact force and pressure for a 25-storey building. Using the center height and distance from the blast source, the scaled distance (Z) is computed. Blast pressure (Pro) multiplied by floor area yields the force on each floor. Lower floors (1–21) experience uniform force (216 kN, 80 kN/m²), while upper floors (22–25) show increased pressure (100–110 kN/m²) and forces (250–264 kN), highlighting the amplified blast effects at higher elevations.

VII. Models in ETABS irregular

G+15 Regular and Irregular

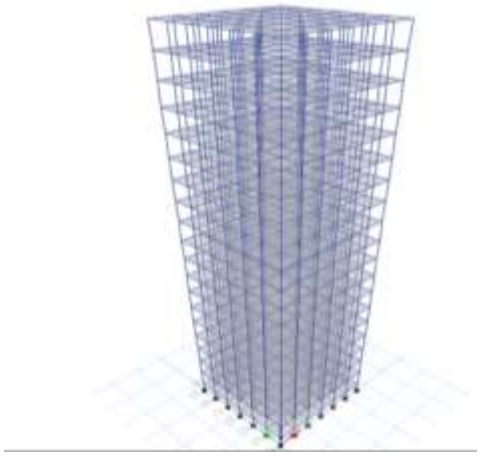

Figure 4: D Structural Frame Model of a High-Rise Building

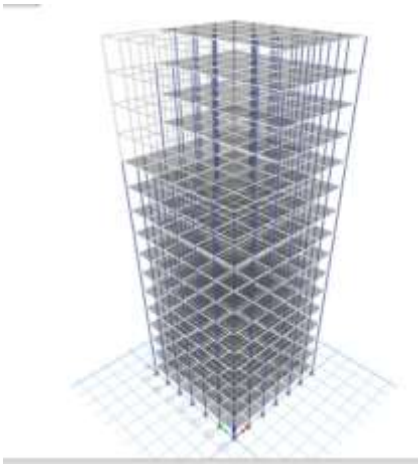

Figure 5: 3D Structural Model of the G+15 Building

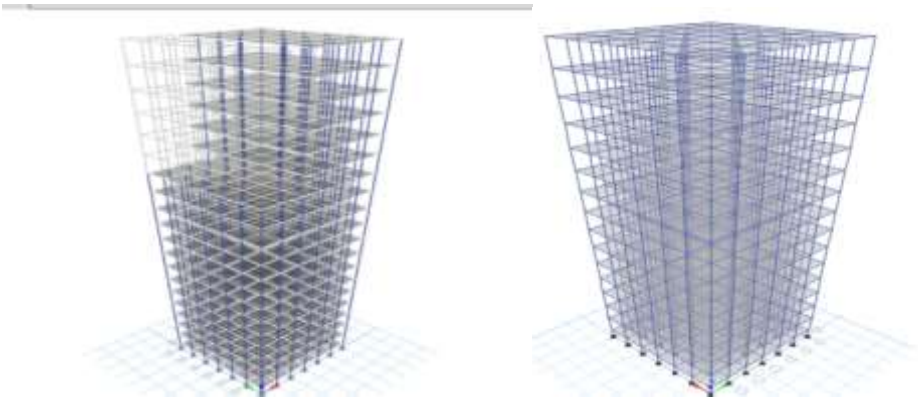

Figure 6: 3D and Elevation View of the Structural Model in ETABS

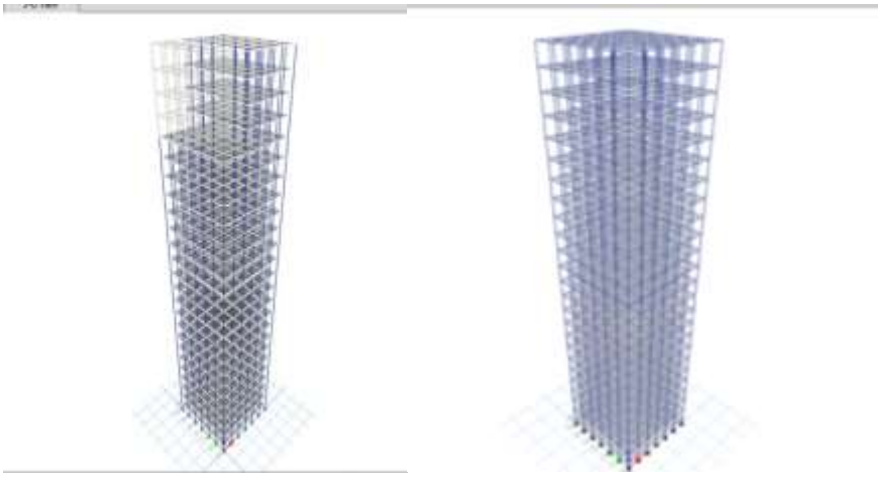

Figure 7: 3D Structural Model of High-Rise Building

VIII. RESULT AND DESCUSSION

G+15

The table 6 presents the deformation values for various TNT explosion scenarios (100 kg TNT) at different distances (10m, 15m, and 20m) and blast types (regular and irregular) across 15 storeys. The deformation values show a general decreasing trend as the distance from the explosion increases, with irregular blasts leading to slightly higher deformations compared to regular blasts. The deformation is highest at 10m and decreases with distance, indicating a reduction in impact with increasing proximity to the explosion source.

Table 6: Impact of TNT Explosion at Different Distances on Structural Deformation Across Storeys

STOREY NO.	100kg TNT 10m REGULAR	100kg TNT 10m IRREGULAR	100kg TNT 15m REGULAR	100kg TNT 15m IRREGULAR	100kg TNT 20m REGULAR	100kg TNT 20m IRREGULAR
1	0.0863	0.0875	0.0751	0.0738	0.0601	0.0579
2	0.0863	0.0889	0.0751	0.0742	0.0601	0.0596
3	0.0818	0.0819	0.0712	0.0703	0.0569	0.0551
4	0.0863	0.0867	0.0751	0.0707	0.0601	0.0629
5	0.0841	0.086	0.0731	0.076	0.0585	0.0616
6	0.0818	0.0823	0.0712	0.0744	0.0569	0.0549
7	0.0841	0.0848	0.0731	0.0759	0.0585	0.0597
8	0.0818	0.0833	0.0712	0.0679	0.0569	0.0539
9	0.0774	0.0812	0.0673	0.0639	0.0538	0.0519
10	0.0774	0.0804	0.0673	0.0678	0.0538	0.0566
11	0.0774	0.0813	0.0673	0.0685	0.0538	0.0569
12	0.0825	0.0776	0.0718	0.0737	0.0574	0.0564
13	0.0825	0.0856	0.0718	0.075	0.0574	0.0594
14	0.0825	0.0828	0.0718	0.0758	0.0574	0.0572
15	0.0825	0.0826	0.0718	0.0675	0.0574	0.0559

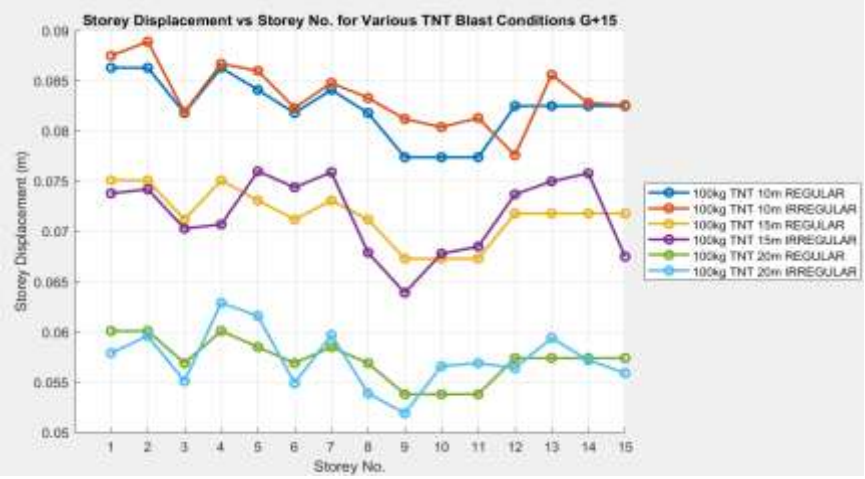

Figure 8: Storey Displacement vs Storey No. for Various TNT Blast Conditions G+15

The figure 8 shows the displacement of different storeys (1 to 15) under various TNT blast conditions (100kg TNT at different distances of 10m, 15m, and 20m for both regular and irregular conditions). The storey displacement is highest for the 100kg TNT at 10m in regular conditions, while the displacement decreases as the distance from the blast increases, with the lowest displacements observed at 20m under both regular and irregular blast conditions. The pattern of displacement fluctuations across the storeys is consistent, with slight variations as the blast distance changes.

Table 7 presents deformation values for 100 kg TNT blasts at 10 m, 15 m, and 20 m under both regular and irregular conditions across 15 storeys. Deformation increases with storey height, peaking at the 15th storey. Irregular blasts produce higher deformations than regular ones, while increasing standoff distance reduces deformation. The data demonstrates a clear correlation between blast intensity, irregularity, distance, and structural response at different storey levels.

Table 7 Deformation of Structural Members under TNT Blast Load at Different Distances Across Storeys

STOREY NO.	100kg TNT 10m REGULAR	100kg TNT 10m IRREGULAR	100kg TNT 15m REGULAR	100kg TNT 15m IRREGULAR	100kg TNT 20m REGULAR	100kg TNT 20m IRREGULAR
1	0.002	0.001	0.001	0.005	0.002	0.002
2	0.004	0.003	0.002	0.011	0.005	0.004
3	0.006	0.004	0.003	0.016	0.007	0.006
4	0.009	0.006	0.003	0.022	0.01	0.007
5	0.011	0.007	0.004	0.027	0.012	0.009
6	0.013	0.008	0.005	0.032	0.015	0.011
7	0.015	0.01	0.006	0.038	0.017	0.013
8	0.017	0.011	0.007	0.043	0.02	0.015
9	0.019	0.013	0.008	0.049	0.022	0.017
10	0.021	0.014	0.009	0.054	0.025	0.019
11	0.023	0.015	0.01	0.059	0.027	0.021
12	0.026	0.017	0.01	0.065	0.03	0.022
13	0.028	0.018	0.011	0.07	0.032	0.024
14	0.03	0.02	0.012	0.076	0.035	0.026
15	0.032	0.021	0.013	0.081	0.037	0.028

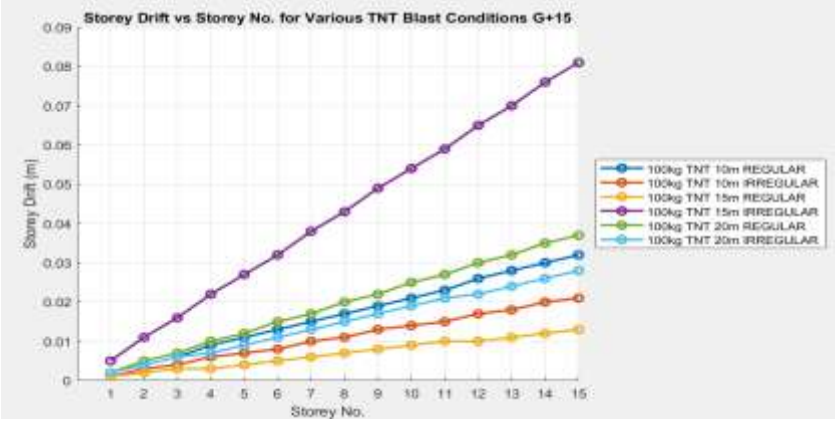

Figure 9: Storey Drift vs Storey No. for Various TNT Blast Conditions G+15

The figure 9 illustrates the storey drift in response to varying TNT blast conditions at different distances (10m, 15m, and 20m) for a 100kg TNT explosion. It shows an increase in drift with the height of the building (storey number). For each distance, regular blast conditions exhibit higher storey drifts compared to irregular ones, with the drift magnitude rising with proximity to the explosion.

Table 8 presents deformation responses of various storeys under 100 kg TNT blasts at 10 m, 15 m, and 20 m for both regular and irregular conditions. Deformation is highest at the 1st storey and decreases with height. Irregular blasts consistently produce slightly greater deformation than regular ones, while increasing standoff distance reduces overall impact. The table highlights a consistent trend of higher structural responses at lower storeys and under irregular blast conditions across all distances.

Table 8 Structural Response to TNT Blast Loads at Various Standoff Distances and Blast Types

Standoff	100kg TNT 10m STANDOFF	100kg TNT 10m STANDOFF	100kg TNT 15m STANDOFF	100kg TNT 15m STANDOFF	100kg TNT 20m STANDOFF	100kg TNT 20m STANDOFF
STOREY NO.	REGULAR	IRREGULAR	REGULAR	IRREGULAR	REGULAR	IRREGULAR
1	172.67	175.04	150.15	147.52	120.12	115.71
2	172.67	177.79	150.15	148.49	120.12	119.21
3	163.7	163.76	142.35	140.67	113.88	110.24
4	172.67	173.5	150.15	141.5	120.12	125.79
5	168.19	172.07	146.25	151.9	117	123.24
6	163.7	164.55	142.35	148.72	113.88	109.86
7	168.19	169.55	146.25	151.86	117	119.47
8	163.7	166.69	142.35	135.8	113.88	107.71
9	154.73	162.35	134.55	127.73	107.64	103.82
10	154.73	160.76	134.55	135.68	107.64	113.11
11	154.73	162.6	134.55	136.92	107.64	113.75
12	165.08	155.25	143.55	147.44	114.84	112.8
13	165.08	171.1	143.55	150.02	114.84	118.88
14	165.08	165.69	143.55	151.52	114.84	114.48
15	165.08	165.26	143.55	135.07	114.84	111.83

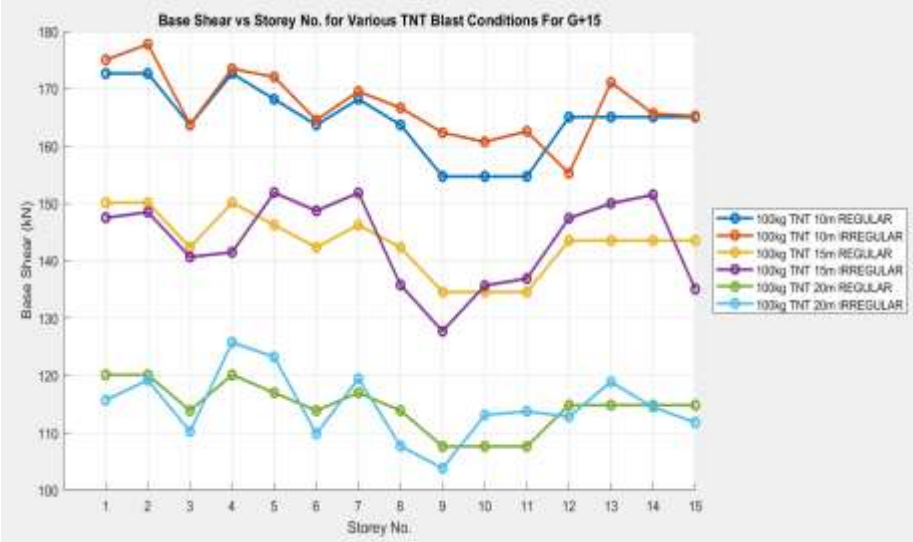

Figure 10: Base Shear vs Storey No. for Various TNT Blast Conditions for G+15

The figure 10 illustrates the variation in base shear across different storeys (1 to 15) for various TNT blast conditions (100kg TNT at 10m, 15m, and 20m standoff distances) under regular and irregular scenarios. It shows that the base shear increases with the proximity of the blast (shorter standoff distance) and the irregularity of the structure. The base shear is highest for the 100kg TNT at 10m regular and irregular conditions, indicating more significant forces acting on the building closer to the blast.

G+20

Table 9 presents deformation values for 100 kg TNT blasts at 10 m, 15 m, and 20 m across 20 storeys under both regular and irregular conditions. Deformation is highest at the 1st storey and decreases with storey height. Irregular blasts consistently produce slightly greater deformation than regular blasts. Increasing standoff distance reduces the overall deformation, highlighting the inverse relationship between blast distance and structural impact, with irregular blasts causing marginally higher responses at all distances.

Table 9 Deformation of Structural Members Under TNT Blast Load at Varying Distances and Blast Types Across Storeys

STOREY NO.	100kg TNT 10m REGULAR	100kg TNT 10m IRREGULAR	100kg TNT 15m REGULAR	100kg TNT 15m IRREGULAR	100kg TNT 20m REGULAR	100kg TNT 20m IRREGULAR
1	0.0924	0.0886	0.0781	0.0765	0.0613	0.0611
2	0.0928	0.0919	0.0787	0.0778	0.0618	0.0631
3	0.0884	0.0866	0.0748	0.0767	0.061	0.0615
4	0.0841	0.086	0.0735	0.0725	0.0619	0.0591
5	0.0906	0.0913	0.0786	0.0759	0.0607	0.0665
6	0.0891	0.0881	0.0786	0.0793	0.0599	0.0669
7	0.0897	0.0869	0.0746	0.0769	0.0589	0.0627
8	0.0843	0.0884	0.0723	0.0799	0.0609	0.059
9	0.0877	0.0912	0.0755	0.0775	0.059	0.0624
10	0.0844	0.0887	0.0742	0.0763	0.0591	0.0581
11	0.0848	0.0875	0.0735	0.0708	0.0599	0.0568
12	0.0786	0.0835	0.07	0.0677	0.0572	0.0549

13	0.0799	0.0838	0.071	0.0714	0.056	0.0567
14	0.0783	0.0829	0.0682	0.0691	0.0545	0.0588
15	0.0808	0.0827	0.0707	0.0742	0.0578	0.0587
16	0.0833	0.0831	0.073	0.079	0.0589	0.0607
17	0.0888	0.0887	0.0734	0.0788	0.0596	0.0597
18	0.0862	0.0906	0.0744	0.0798	0.0583	0.0618
19	0.0874	0.0879	0.0746	0.0773	0.0613	0.0582
20	0.0839	0.0835	0.0728	0.072	0.0588	0.057

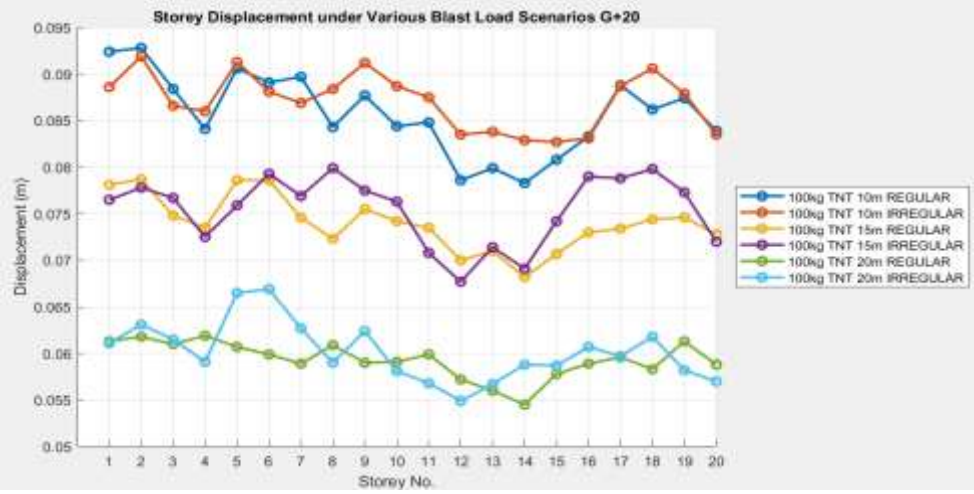

Figure 11: Storey Displacement under Various Blast Load Scenarios G+20

Figure 11 illustrates storey displacement under 100 kg TNT blasts at 10 m, 15 m, and 20 m for regular and irregular scenarios. Displacement increases at closer distances, with irregular blasts causing greater movement. Peak displacements occur at specific storeys, highlighting varying structural responses and greater vulnerability under irregular blast conditions.

Table 10 presents deformation values for structural members under 100 kg TNT explosions at 10 m, 15 m, and 20 m across 20 storeys, for both regular and irregular blasts. Deformation increases with storey height, peaking at the 20th storey. Higher deformations occur at closer distances (10 m), decreasing with increased standoff. Irregular blasts consistently produce slightly greater deformation than regular ones, reflecting the stronger impact of irregular blast forces, particularly near the source.

Table 10 Deformation Response of Structural Members Under TNT Blast Load at Varying Distances and Blast Types Across Storeys

STOREY NO.	100kg TNT 10m REGULAR	100kg TNT 10m IRREGULAR	100kg TNT 15m REGULAR	100kg TNT 15m IRREGULAR	100kg TNT 20m REGULAR	100kg TNT 20m IRREGULAR
1	0.002	0.0013	0.001	0.0051	0.0021	0.0025
2	0.0042	0.0031	0.0021	0.0109	0.0047	0.005
3	0.0065	0.0049	0.0031	0.0166	0.0072	0.0076
4	0.0093	0.0067	0.0041	0.0224	0.0098	0.01
5	0.012	0.0085	0.0052	0.0281	0.0123	0.0125
6	0.0146	0.0104	0.0063	0.0338	0.0149	0.015

7	0.0171	0.0122	0.0074	0.0395	0.0174	0.0175
8	0.0197	0.014	0.0085	0.0452	0.02	0.02
9	0.0225	0.016	0.0096	0.0509	0.0226	0.0226
10	0.0252	0.0178	0.0107	0.0566	0.0251	0.0251
11	0.028	0.0197	0.0118	0.0623	0.0277	0.0277
12	0.0309	0.0215	0.0129	0.068	0.0302	0.0302
13	0.0338	0.0234	0.014	0.0737	0.0328	0.0328
14	0.0366	0.0252	0.0151	0.0794	0.0353	0.0353
15	0.0395	0.0271	0.0162	0.0851	0.0379	0.0379
16	0.0422	0.0289	0.0172	0.0908	0.0404	0.0404
17	0.0449	0.0308	0.0183	0.0965	0.043	0.043
18	0.0476	0.0326	0.0194	0.1022	0.0455	0.0455
19	0.0503	0.0344	0.0205	0.1079	0.0481	0.0481
20	0.053	0.0363	0.0216	0.1136	0.0506	0.0506

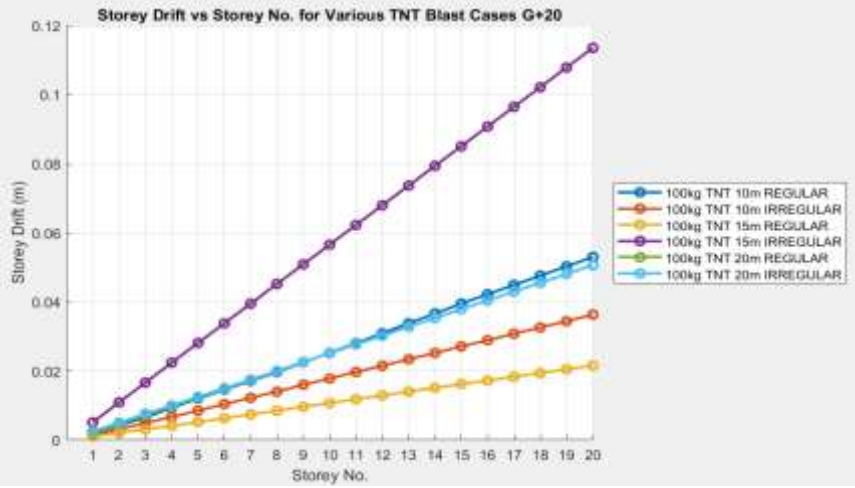

Figure 12: Storey Drift vs Storey No. for Various TNT Blast Cases G+20

This figure 12 illustrates the storey drift of a building in response to TNT blast loads at different distances (10m, 15m, and 20m) and blast scenarios (regular and irregular). The storey drift increases with the number of storeys, and the drift is more pronounced for TNT at closer distances (10m), especially under irregular blast conditions. Irregular blasts consistently result in higher drift compared to regular blasts across all distances.

The table 11 presents the deformation (in mm) of various storeys subjected to a 100kg TNT explosion at different standoff distances (10m, 15m, and 20m) for both regular and irregular blast scenarios. The deformation generally decreases with increased standoff distance, with the highest values occurring at 10m standoff distance, particularly for the regular explosion scenario. As the standoff distance increases, the blast impact on storey deformation diminishes, reflecting the reduced intensity of shockwaves at greater distances.

Table 11: Storey Deformation under TNT Explosion Impact at Different Standoff Distances

STOREY NO.	100kg TNT 10m STANDOFF - REGULAR	100kg TNT 10m STANDOFF - IRREGULAR	100kg TNT 15m STANDOFF - REGULAR	100kg TNT 15m STANDOFF - IRREGULAR	100kg TNT 20m STANDOFF - REGULAR	100kg TNT 20m STANDOFF - IRREGULAR
1	172.67	175.04	150.15	147.52	120.12	115.71
2	172.67	177.79	150.15	148.49	120.12	119.21
3	163.7	163.76	142.35	140.67	113.88	110.24
4	172.67	173.5	150.15	141.5	120.12	125.79
5	168.19	172.07	146.25	151.9	117	123.24
6	163.7	164.55	142.35	148.72	113.88	109.86
7	168.19	169.55	146.25	151.86	117	119.47
8	163.7	166.69	142.35	135.8	113.88	107.71
9	154.73	162.35	134.55	127.73	107.64	103.82
10	154.73	160.76	134.55	135.68	107.64	113.11
11	154.73	162.6	134.55	136.92	107.64	113.75
12	165.08	155.25	143.55	147.44	114.84	112.8
13	165.08	171.1	143.55	150.02	114.84	118.88
14	165.08	165.69	143.55	151.52	114.84	114.48
15	165.08	165.26	143.55	135.07	114.84	111.83
16	161.78	164	140.68	142.63	112.54	112.76
17	158.48	160.66	137.81	139.72	110.25	110.46
18	155.18	157.31	134.94	136.8	107.95	108.16
19	151.87	153.96	132.07	133.89	105.65	105.86
20	148.57	150.62	129.2	130.98	103.36	103.56

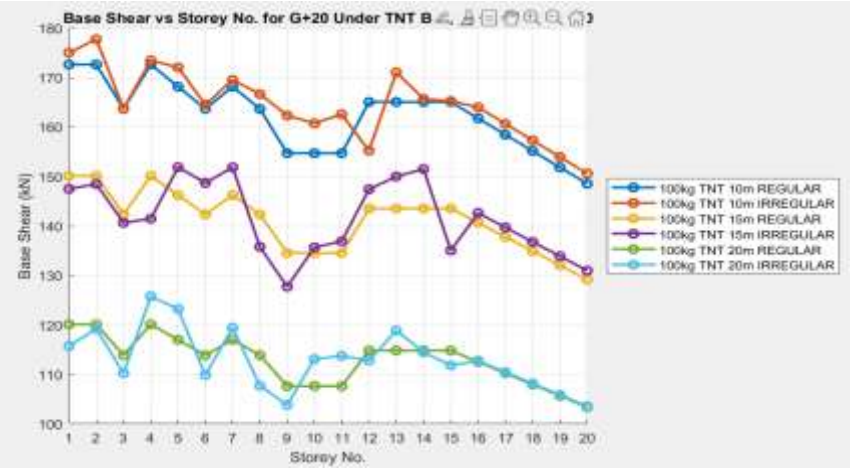

Figure 13: Base Shear vs Storey Number for G+20 Under TNT B.

This figure 13 illustrates the variation in base shear across different storey numbers of a G+20 structure under TNT explosion loading at varying distances. The base shear decreases with increasing storey number, and there is a noticeable difference between the regular and irregular configurations for different TNT distances (10m, 15m, and 20m). Regular configurations generally exhibit higher base shear values compared to irregular configurations. Additionally, as the TNT distance increases, the base shear values tend to decrease across all configurations.

G+25

Table 12 shows storey displacements (m) under a 100 kg TNT explosion at 10 m, 15 m, and 20 m standoff distances for both regular and irregular blasts. Displacement decreases with increasing distance, with maximum values at 10 m. Irregular blasts produce slightly higher displacements than regular ones, highlighting stronger shockwave effects, especially on lower storeys.

Table 12: Storey Displacement under TNT Explosion Impact at Different Standoff Distances

STOREY NO.	100kg TNT 10m REGULAR	100kg TNT 10m IRREGULAR	100kg TNT 15m REGULAR	100kg TNT 15m IRREGULAR	100kg TNT 20m REGULAR	100kg TNT 20m IRREGULAR
1	0.0839	0.0864	0.0704	0.0725	0.0582	0.0599
2	0.0854	0.088	0.0722	0.0744	0.0594	0.0612
3	0.0873	0.0899	0.0711	0.0732	0.0601	0.0619
4	0.0854	0.088	0.0739	0.0761	0.0604	0.0622
5	0.0849	0.0874	0.0724	0.0746	0.0601	0.0619
6	0.0888	0.0915	0.0744	0.0766	0.0603	0.0621
7	0.0893	0.092	0.0743	0.0765	0.0609	0.0627
8	0.0893	0.092	0.0748	0.077	0.062	0.0639
9	0.0913	0.094	0.0747	0.0769	0.0621	0.064
10	0.0905	0.0932	0.0755	0.0778	0.0626	0.0645
11	0.0902	0.0929	0.0777	0.08	0.0631	0.065
12	0.0903	0.093	0.079	0.0814	0.0637	0.0656
13	0.092	0.0948	0.0774	0.0797	0.0634	0.0653
14	0.0944	0.0972	0.0784	0.0808	0.0654	0.0674
15	0.0918	0.0946	0.0784	0.0808	0.064	0.0659
16	0.0946	0.0974	0.0812	0.0836	0.0664	0.0684
17	0.097	0.0999	0.0821	0.0846	0.067	0.069
18	0.0943	0.0971	0.0824	0.0849	0.0661	0.0681
19	0.0971	0.1	0.0811	0.0835	0.0665	0.0685
20	0.0973	0.1002	0.0818	0.0843	0.0681	0.0701
21	0.0987	0.1017	0.0825	0.085	0.0681	0.0701
22	0.0973	0.1002	0.084	0.0865	0.0683	0.0703
23	0.101	0.104	0.0838	0.0863	0.069	0.0711
24	0.0997	0.1027	0.085	0.0876	0.0692	0.0713
25	0.1008	0.1038	0.0839	0.0864	0.0706	0.0727

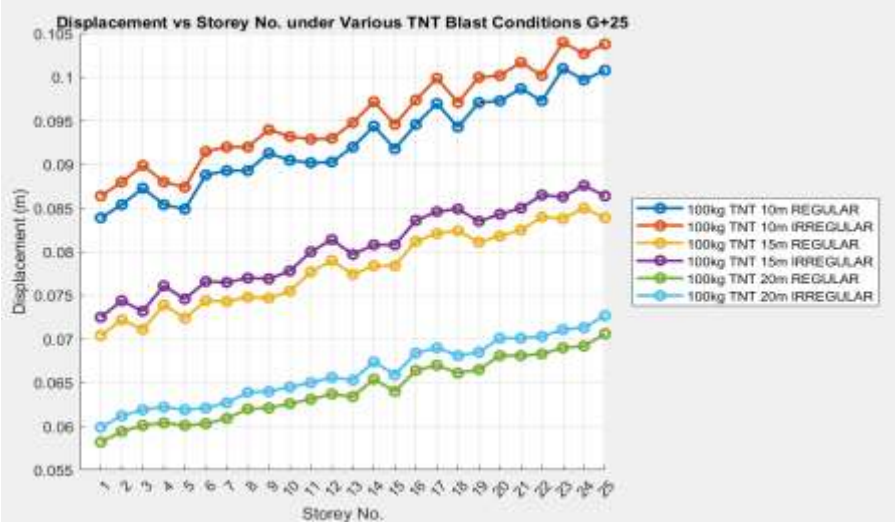

Figure 14: Displacement vs Storey No. under Various TNT Blast Conditions G+25

Figure 14 illustrates storey-wise displacement under 100 kg TNT blasts at 10 m, 15 m, and 20 m for both regular and irregular scenarios. Displacement increases with storey height and is more pronounced in irregular blasts, particularly at 10 m. The trend highlights the effect of blast intensity and proximity on structural deformation.

Table 13 presents maximum storey accelerations (m/s²) under a 100 kg TNT explosion at 10 m, 15 m, and 20 m standoffs. Acceleration decreases with distance, is highest at 10 m, and is slightly greater for irregular blasts. Higher storeys experience increasing acceleration, indicating cumulative shockwave effects on the structure.

Table 13 Storey Maximum Acceleration under TNT Explosion Impact at Different Standoff Distances

STOREY NO.	100kg TNT 10m REGULAR	100kg TNT 10m IRREGULAR	100kg TNT 15m REGULAR	100kg TNT 15m IRREGULAR	100kg TNT 20m REGULAR	100kg TNT 20m IRREGULAR
1	0.0045	0.0038	0.0035	0.0076	0.0046	0.005
2	0.0067	0.0056	0.0046	0.0134	0.0072	0.0075
3	0.009	0.0074	0.0056	0.0191	0.0097	0.0101
4	0.0118	0.0092	0.0066	0.0249	0.0123	0.0125
5	0.0145	0.011	0.0077	0.0306	0.0148	0.015
6	0.0171	0.0129	0.0088	0.0363	0.0174	0.0175
7	0.0196	0.0147	0.0099	0.042	0.0199	0.02
8	0.0222	0.0165	0.011	0.0477	0.0225	0.0225
9	0.025	0.0185	0.0121	0.0534	0.0251	0.0251
10	0.0277	0.0203	0.0132	0.0591	0.0276	0.0276
11	0.0305	0.0222	0.0143	0.0648	0.0302	0.0302
12	0.0334	0.024	0.0154	0.0705	0.0327	0.0327
13	0.0363	0.0259	0.0165	0.0762	0.0353	0.0353
14	0.0391	0.0277	0.0176	0.0819	0.0378	0.0378
15	0.042	0.0296	0.0187	0.0876	0.0404	0.0404
16	0.0447	0.0314	0.0197	0.0933	0.0429	0.0429

17	0.0474	0.0333	0.0208	0.099	0.0455	0.0455
18	0.0501	0.0351	0.0219	0.1047	0.048	0.048
19	0.0528	0.0369	0.023	0.1104	0.0506	0.0506
20	0.0555	0.0388	0.0241	0.1161	0.0531	0.0531
21	0.059	0.042	0.0258	0.1208	0.0562	0.0562
22	0.0622	0.0455	0.0275	0.126	0.0589	0.0594
23	0.0657	0.0483	0.0294	0.1311	0.0618	0.0623
24	0.0684	0.0509	0.0314	0.1361	0.0648	0.0652
25	0.0713	0.0538	0.0332	0.1415	0.068	0.0679

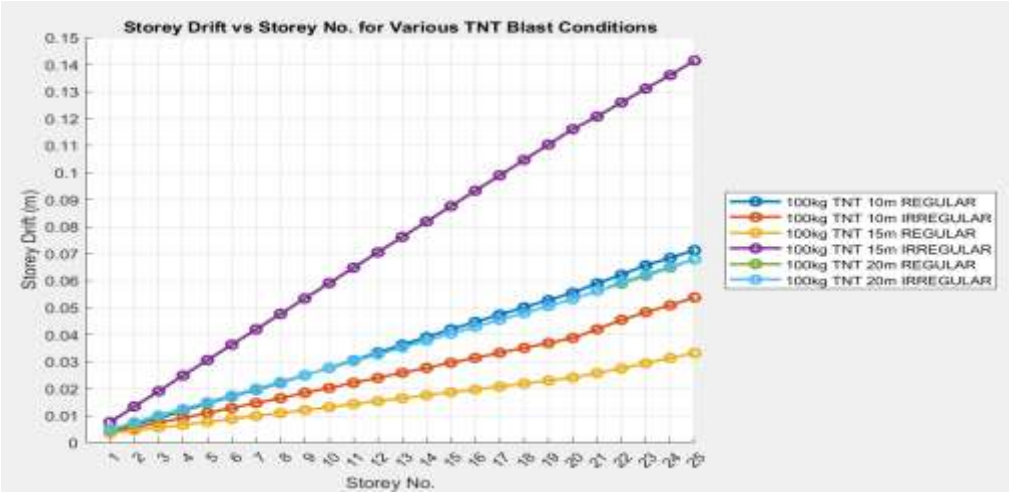

Figure 15: Storey Drift vs Storey No. for Various TNT Blast Conditions

Figure 15 depicts storey drift versus storey number under 100 kg TNT blasts at 10 m, 15 m, and 20 m for regular and irregular conditions. Drift increases with storey height, rising more sharply under irregular blasts. Greater TNT quantities and closer distances produce higher drifts, highlighting the combined effect of blast intensity and type on structural deformation.

Table 14 shows storey-wise displacements (mm) under a 100 kg TNT explosion at standoff distances of 10 m, 15 m, and 20 m for both regular and irregular blasts. Displacement decreases as standoff distance increases, with the highest values at 10 m. Irregular blasts consistently produce slightly higher displacements than regular ones. Lower storeys experience greater movement, while upper storeys show reduced deformation. This highlights the inverse relationship between standoff distance and structural displacement, with irregular explosions causing marginally more deformation.

Table 14: Storey Displacement under TNT Explosion Impact at Different Standoff Distances (Impact in mm)

STOREY NO.	100kg TNT 10m STANDOFF - REGULAR	100kg TNT 10m STANDOFF - IRREGULAR	100kg TNT 15m STANDOFF - REGULAR	100kg TNT 15m STANDOFF - IRREGULAR	100kg TNT 20m STANDOFF - REGULAR	100kg TNT 20m STANDOFF - IRREGULAR
1	175.4	180.34	152.53	152.54	122.02	122.18
2	171.52	176.89	149.15	150	119.32	120.66
3	168.47	174.15	146.5	148.07	117.2	119.48
4	166.16	172.04	144.49	146.69	115.59	118.59

5	164.48	170.48	143.03	145.77	114.42	117.95
6	163.34	169.37	142.04	145.23	113.63	117.5
7	162.64	168.63	141.43	145	113.14	117.22
8	162.29	168.19	141.12	144.99	112.9	117.04
9	162.18	167.95	141.03	145.14	112.82	116.93
10	162.22	167.82	141.06	145.36	112.85	116.84
11	162.31	167.73	141.14	145.58	112.91	116.72
12	162.35	167.59	141.18	145.71	112.94	116.55
13	162.25	167.31	141.09	145.68	112.87	116.25
14	161.91	166.81	140.79	145.41	112.63	115.8
15	161.22	166	140.2	144.83	112.16	115.15
16	160.1	164.8	139.22	143.85	111.38	114.26
17	158.45	163.13	137.78	142.4	110.22	113.07
18	156.16	160.89	135.79	140.4	108.63	111.55
19	153.14	158.01	133.17	137.77	106.53	109.64
20	149.29	154.4	129.83	134.43	103.86	107.32
21	144.52	149.97	125.68	130.31	100.54	104.52
22	138.72	144.64	120.64	125.33	96.51	101.21
23	131.81	138.32	114.63	119.41	91.7	97.34
24	123.67	130.94	107.56	112.47	86.04	92.86
25	114.22	122.39	99.34	104.43	79.47	87.74

Figure 16: Base Shear vs Storey No. for G+25 under TNT Blast Conditions

This figure 16 presents the base shear (in kN) versus storey number for a G+25 building subjected to various TNT blast conditions. The graph shows that the base shear decreases as the storey number increases, with the irregular blast conditions (represented by orange, purple, and green lines) causing higher base shear values compared to regular blast conditions (represented by blue, purple,

and green lines). Additionally, the TNT blast intensity (10m, 15m, 20m stand-off distances) has a noticeable impact, with closer stand-off distances (10m) resulting in higher base shear forces.

Time and Frequency

Cases	Max time (sec)	Front Face Max Load (kN/m²)
100kg @ 30m	0.0058	150.15

Table 15 presents the mode shapes, corresponding time periods, and frequencies for the analyzed building. As the mode number increases from 1 to 15, the time period decreases from 1.2 s to 0.22 s, indicating faster vibration cycles for higher modes. Correspondingly, the frequency increases from 0.833 Hz to 4.545 Hz. This trend reflects the building's dynamic behavior, with higher modes contributing to localized vibrations and influencing seismic and blast response characteristics.

Table 15: Mode Shape, Time Period, and Frequency Data

Mode Shape No	Time period (sec)	Frequency
1	1.2	0.833
2	1.13	0.885
3	1.06	0.943
4	0.99	1.01
5	0.92	1.087
6	0.85	1.176
7	0.78	1.282
8	0.71	1.408
9	0.64	1.562
10	0.57	1.754
11	0.5	2
12	0.43	2.326
13	0.36	2.778
14	0.29	3.448
15	0.22	4.545

Table 16 summarizes the mode shapes, time periods, and corresponding frequencies for the second set of building analyses. The time period decreases from 1.3 s (mode 1) to 0.255 s (mode 20), while the frequency increases from 0.769 Hz to 3.922 Hz. This demonstrates that higher modes vibrate faster and are associated with localized structural responses. Such data are critical for understanding dynamic characteristics and predicting building behavior under seismic and blast loads.

Table 16: Mode Shape, Time Period, and Frequency Data (Second Set)

Mode Shape No	Time period (sec)	Frequency
1	1.3	0.769
2	1.245	0.803
3	1.19	0.84
4	1.135	0.881
5	1.08	0.926

6	1.025	0.976
7	0.97	1.031
8	0.915	1.093
9	0.86	1.163
10	0.805	1.242
11	0.75	1.333
12	0.695	1.439
13	0.64	1.562
14	0.585	1.709
15	0.53	1.887
16	0.475	2.105
17	0.42	2.381
18	0.365	2.74
19	0.31	3.226
20	0.255	3.922

Table 17 presents the mode shapes, time periods, and frequencies for the third set of building models. The time period gradually decreases from 1.4 s (mode 1) to 0.248 s (mode 25), while the frequency increases from 0.714 Hz to 4.032 Hz. This indicates that higher modes correspond to faster, localized vibrations, highlighting the building's dynamic characteristics. Such analysis is essential for evaluating seismic and blast responses and designing structures to withstand dynamic loads effectively.

Table 17: Mode Shape, Time Period, and Frequency Data (Third Set)

Mode Shape No	Time period (sec)	Frequency
1	1.4	0.714
2	1.352	0.74
3	1.304	0.767
4	1.256	0.796
5	1.208	0.828
6	1.16	0.862
7	1.112	0.899
8	1.064	0.94
9	1.016	0.984
10	0.968	1.033
11	0.92	1.087
12	0.872	1.147

13	0.824	1.214
14	0.776	1.289
15	0.728	1.374
16	0.68	1.471
17	0.632	1.582
18	0.584	1.712
19	0.536	1.866
20	0.488	2.049
21	0.44	2.273
22	0.392	2.551
23	0.344	2.907
24	0.296	3.378
25	0.248	4.032

IX. CONCLUSION

This research investigates the dynamic response and blast resistance of vertical irregular reinforced concrete (RCC) buildings, specifically G+15, G+20, and G+25 structures with soft-storey configurations. The study emphasizes the vulnerabilities introduced by vertical irregularities, particularly soft storeys, which significantly influence the structural response under blast loading. Through detailed Finite Element Analysis (FEA) and time-history simulations in ETABS, the impact of varying TNT blast scenarios at different standoff distances was examined, highlighting the critical effects of proximity, irregularity, and storey height on displacement, inter-storey drift, and base shear. The results indicate that irregular structures consistently experience higher deformations and drifts compared to regular ones, with the maximum impact observed at lower standoff distances. Soft-storey floors exhibited pronounced lateral displacements, confirming their susceptibility to progressive failure under dynamic impulsive forces. The study also demonstrates that increasing the standoff distance substantially reduces the intensity of blast-induced forces, while the inclusion of structural reinforcements such as shear walls and optimized reinforcement detailing can mitigate potential damage. Overall, the research underscores the necessity of considering blast loads alongside conventional gravity and seismic forces in the design of high-rise buildings, particularly in high-risk or sensitive areas. The findings contribute valuable insights for structural engineers and designers by identifying critical weaknesses, offering design modifications, and emphasizing resilience-focused strategies. By addressing the challenges posed by vertical irregularities and soft-storey conditions, this study provides a foundation for enhancing the blast resistance and overall safety of reinforced concrete high-rise structures, ensuring structural integrity and occupant protection during extreme dynamic events.

X. FUTURE SCOPE

The present study on the blast resistance of vertical irregular RCC buildings provides a foundation for several future research directions. Firstly, incorporating multi-hazard scenarios—such as simultaneous seismic and blast loading—can offer a more realistic assessment of structural resilience under extreme events. Further research could explore advanced material technologies, including high-performance concrete, fiber-reinforced polymers, or smart composites, to enhance blast resistance and energy dissipation capacity. The current analysis focuses on specific standoff distances and TNT equivalents; future studies can expand this by evaluating a broader range of explosive intensities, directions, and irregular geometries, including asymmetrical plan and elevation configurations. Optimization techniques, such as topology optimization or performance-based design approaches, could be applied to identify the most efficient reinforcement and structural layout for blast mitigation. Integration of real-time monitoring systems with structural health sensors and AI-based predictive models can further improve safety by enabling early warning and adaptive response strategies. Additionally, experimental validation through scaled model testing or hybrid simulation can complement numerical findings, enhancing the reliability of design recommendations. These advancements will contribute to developing resilient, safe, and cost-effective high-rise structures capable of withstanding dynamic hazards effectively.

References

[1] K. M. Ro, M. S. Kim, and Y. H. Lee, "A simplified approach to modeling vertically irregular structures for dynamic assessment," *Journal of Asian Architecture and Building Engineering*, vol. 21, no. 6, pp. 2320–2329, Nov. 2022, doi: 10.1080/13467581.2021.1971682.

[2] S. Ruggieri and G. Uva, "Accounting for the Spatial Variability of Seismic Motion in the Pushover Analysis of Regular and Irregular RC Buildings in the New Italian Building Code," *Buildings*, vol. 10, no. 10, p. 177, Oct. 2020, doi: 10.3390/buildings10100177.

[3] M. G. Mungalkar and I. Dahat, "ASSESSING VERTICAL IRREGULARITY IN BUILDINGS ACROSS SEISMIC ZONES: A COMPARATIVE STUDY," vol. 04, no. 06, 2024.

[4] S. Akhil Ahamad and K. V. Pratap, "Dynamic analysis of G + 20 multi storied building by using shear walls in various locations for different seismic zones by using Etabs," *Materials Today: Proceedings*, vol. 43, pp. 1043–1048, 2021, doi: 10.1016/j.matpr.2020.08.014.

[5] M. Modi, "Dynamic Analysis of RC Building having Vertical Irregularity," vol. 6, no. 7.

[6] H. Akhilesh and B. Naveen, "Dynamic Analysis of Vertical Irregular Tall Structural System," *IOP Conf. Ser.: Mater. Sci. Eng.*, vol. 1006, no. 1, p. 012021, Dec. 2020, doi: 10.1088/1757-899X/1006/1/012021.

[7] N. A. N. Zainab, W. H. Tan, W. Faridah, A. M. Andrew, S. Ragunathan, and A. S. N. Amirah, "Evaluate the Performance of Regular and Irregular Shape of Building Based on Dynamic Analysis," in *Intelligent Manufacturing and Mechatronics*, M. S. Bahari, A. Harun, Z. Zainal Abidin, R. Hamidon, and S. Zakaria, Eds., in Lecture Notes in Mechanical Engineering. , Singapore: Springer Singapore, 2021, pp. 651–660. doi: 10.1007/978-981-16-0866-7_55.

[8] "[No title found]," *IRJMETS*.

[9] A. Koçak, B. Zengin, and F. Kadioğlu, "Performance assessment of irregular RC buildings with shear walls after Earthquake," *Engineering Failure Analysis*, vol. 55, pp. 157–168, Sept. 2015, doi: 10.1016/j.engfailanal.2015.05.016.

[10] D. Annapurna, E. Yaqubi, P. Anuradha, and K. L. Radhika, "Seismic response of RC framed irregular structures," *Materials Today: Proceedings*, vol. 93, pp. 530–537, 2023, doi: 10.1016/j.matpr.2023.09.028.

[11] S. Nikale and S. Salve, "STRUCTURAL ASSESSMENT OF REGULAR AND IRREGULAR BUILDING DESIGNS: A REVIEW," vol. 12, no. 7, 2025.

[12] S. G, Dr. R. S. C. Bose, and Dr. G. H S, "Study on Dynamic Behavior of Shear Walls in Vertically Irregular Building Frames," *IJRASET*, vol. 10, no. 7, pp. 1339–1351, July 2022, doi: 10.22214/ijraset.2022.45311.